Organic & Biomolecular Chemistry

ROYAL SOCIETY OF CHEMISTRY

PAPER

View Article Online
View Journal

Cite this: DOI: 10.1039/d5ob01062d

Anti-adipogenic effects of *N*-acetyltyramine from termite-associated *Streptomyces* sp. M45

Se Yun Jeong,†[a] Mei Tong He,†[b] Mihyang Kim, †[c] Ki-Hwan Nam,[d] Michael Poulsen, [e] Christine Beemelmanns, [f,g] Ki Sung Kang*[b] and Ki Hyun Kim *[a]

Received 30th June 2025,
Accepted 4th August 2025

DOI: 10.1039/d5ob01062d

rsc.li/obc

Obesity remains a global health challenge, and novel small-molecule modulators of adipogenesis are urgently needed. Here, we investigated the anti-adipogenic potential of metabolites isolated from termite-associated *Streptomyces* sp. M45. Chemical investigation of the extract from cultured *Streptomyces* sp. M45 led to the isolation of six metabolites (**1–6**). Structures were determined as 2-acetamido-3-hydroxybenzoic acid (**1**), *N*-acetyltyramine (**2**), deoxyuridine (**3**), cyclo(L-Pro-L-Leu) (**4**), cyclo(L-Pro-D-Leu) (**5**), and cyclo(L-Pro-L-Phe) (**6**) *via* comprehensive analysis of nuclear magnetic resonance (NMR) spectroscopy and liquid chromatography–mass spectrometry (LC–MS) data. Notably, the structure of the anthranilic acid derivative, 2-acetamido-3-hydroxybenzoic acid (**1**), was fully elucidated by 1D and 2D NMR, high-resolution electrospray ionization mass spectrometry (HR-ESIMS), and DP4$^+$ probability calculations, allowing us to correct previously reported ^{1}H NMR resonances and to assign ^{13}C NMR signals for the first time. Compounds **1–6** were evaluated for anti-adipogenic activity in differentiated 3T3-L1 cells by assessing lipid accumulation and the expression of adipogenic transcription factors (C/EBPα, C/EBPβ, and SREBP2). Among these, *N*-acetyltyramine (**2**) significantly inhibited adipocyte differentiation without impairing cell viability. Mechanistically, compound **2** downregulated the expression of key adipogenic genes including C/EBPα, SREBP2, FASN, UCP2, and leptin. These findings substantiate its potential as a modulator of obesity-related pathways in 3T3-L1 adipocytes.

Introduction

Obesity is a multifactorial disorder that both accompanies and precipitates components of metabolic syndrome, including type 2 diabetes mellitus, hypertension, cardiovascular disease, and rheumatic conditions.[1] It arises when caloric intake exceeds expenditure, leading to adipose tissue expansion *via* adipocyte hypertrophy (increased cell volume) and hyperplasia (increased cell number).[2,3] Adipogenesis in mammals—the combined processes of hypertrophy and hyperplasia—reflects the differentiation of preadipocytes into mature adipocytes and is orchestrated primarily by the transcription factors peroxisome proliferator-activated receptor γ (PPARγ) and CCAAT/enhancer-binding protein α (C/EBPα).[4,5] PPARγ governs lipid storage and mobilization,[6] whereas C/EBPα directly activates genes required for adipocyte differentiation and maintenance of metabolic homeostasis.[3] Lipid synthesis and uptake are further regulated by sterol regulatory element-binding proteins (SREBPs), of which three isoforms exist—SREBP-1a, SREBP-1c, and SREBP-2.[7] SREBP-1 predominantly drives fatty acid biosynthesis, while SREBP-2 promotes cholesterol synthesis; dysregulation of these pathways is implicated in obesity development.[8] Fatty acid synthase (FAS) catalyzes *de novo* fatty acid production and plays a critical role in energy balance and body-weight regulation.[9,10] Consequently, FAS inhibitors are being evaluated as therapeutic agents for obesity, type 2 diabetes, and certain cancers.[11] Moreover, uncoupling proteins UCP2 and UCP3 are integral to lipid metabolism: UCP2-deficient mice fed a high-fat diet exhibit resistance to obesity and maintain a relatively lean phenotype.[12,13]

Ecology-driven chemical analyses of microbial symbionts, combined with LC–MS–based dereplication strategies, have

[a]*School of Pharmacy, Sungkyunkwan University, Suwon 440-746, Republic of Korea. E-mail: khkim83@skku.edu; Fax: +82-31-290-7730; Tel: +82-31-290-7700*
[b]*College of Korean Medicine, Gachon University, Seongnam 13120, Republic of Korea. E-mail: kkang@gachon.ac.kr; Tel: +82-31-750-5402*
[c]*Quality Management and Evaluation Research Division, National Institute of Crop and Food Science, Rural Development Administraion, Suwon 16613, Republic of Korea*
[d]*Center for Scientific Instrumentation, Korea Basic Science Institute, Daejeon, 34133, Republic of Korea*
[e]*Section for Ecology and Evolution, Department of Biology, University of Copenhagen, Universitetsparken 15, 2100 Copenhagen East, Denmark*
[f]*Department Antiinfectives from Microbiota, Helmholtz Institute for Pharmaceutical Research Saarland, Germany*
[g]*Saarland University, 66123 Saarbrücken, Germany*
†These authors contributed equally to this study.

markedly advanced natural product chemistry and yielded unprecedented rates of novel bioactive compound discovery.[14–16] Metabolomic studies of symbionts involved in insect farming have further illuminated the molecular mechanisms underlying symbiotic stability, as well as the biosynthetic pathways responsible for producing antibacterial metabolites.[17–20] Notably, Actinobacteria, including members of the genus *Streptomyces*, have repeatedly emerged as crucial indirect defensive partners within insect agricultural systems,[21,22] showing potent antifungal activity against co-occurring fungi.[21]

Streptomyces species exhibit remarkable diversity in their morphology, physiology, and biochemical capabilities.[23,24] They are especially renowned for producing a vast range of bioactive metabolites—including antibiotics, anticancer agents, enzyme inhibitors, and pigments—and account for the majority of the more than 5000 microbial antibiotics identified since the discovery of penicillin.[25] For example, streptomycin from *S. griseus* remains a cornerstone of tuberculosis therapy and its biosynthetic genes (*str*) have been extensively studied,[26] while monensin from *S. cinnamonensis* exhibits antibacterial, antiparasitic, and antiproliferative activities.[27] Despite this wealth of secondary chemistry, few studies have explored the anti-adipogenic potential of *Streptomyces*-derived metabolites. Emerging evidence suggests certain antibiotics may suppress adipogenesis, offering novel interventions for obesity and diabetes.[28,29] For instance, cineromycin B inhibits 3T3-L1 differentiation *via* early upregulation of negative regulators KLF2 and KLF3,[28] and echinomycin—a hypoxia-inducible factor-1 inhibitor—blocks adipogenesis by disrupting mitotic clonal expansion.[29] These findings highlight the potential of insect-derived *Streptomyces* as a valuable source of anti-adipogenic compounds.

In our quest to discover novel bioactive metabolites from intriguing natural sources,[30–35] we examined potential bioactive metabolites from *Streptomyces* sp. M45 associated with the fungus-farming termite genus *Odontotermes*. Using successive column chromatography and preparative HPLC, guided by LC–MS analysis, we isolated six metabolites (**1–6**) from the extract from cultured *Streptomyces* sp. M45, including an anthranilic acid derivative (**1**) whose complete spectroscopic characterization had not been previously reported. In this study, we fully elucidated the structure of compound **1** by 1D and 2D NMR, high-resolution ESI-MS, and DP4$^+$ probability calculations. All six metabolites were then evaluated for anti-adipogenic activity in differentiated 3T3-L1 cells by measuring lipid accumulation and impact on the expression of key adipogenic transcription factors (C/EBPα, C/EBPβ, and SREBP2). Herein, we report the isolation, structural characterization, and anti-adipogenic evaluation of compounds **1–6**.

Results and discussion

Isolation of natural products

The methanolic solid phase extract of cultured *Streptomyces* sp. M45 (ISP2 medium, 3L) was partitioned successively with *n*-hexane, CH_2Cl_2, EtOAc, and *n*-BuOH to afford four polarity-graded fractions. Detailed chemical investigations of the CH_2Cl_2, EtOAc, and *n*-BuOH fractions were performed using reversed-phase C_{18} silica gel column chromatography, together with preparative and semi-preparative HPLC, all guided by LC/MS analysis. These efforts culminated in the isolation and structural characterization of six metabolites (**1–6**) (Fig. 1).

Structural elucidation of compounds 1–6

Compound **1** was obtained as a white amorphous powder. Its molecular formula, $C_9H_9NO_4$, was established by HR-ESIMS in positive–ion mode, which exhibited an $[M + H]^+$ ion at *m*/*z* 196.0597 (calcd for $C_9H_{10}NO_4$, 196.0604) (Fig. S2). The formula corresponds to six degrees of unsaturation. The ^{1}H NMR spectrum (Table 1) revealed signals characteristic of a 1,2,3-trisubstituted benzene ring: δ_H 7.05 (1H, d, J = 8.0 Hz, H-4), 7.13 (1H, dd, J = 8.0, 7.5 Hz, H-5), and 7.53 (1H, d, J = 7.5 Hz, H-6), together with a methyl singlet at δ_H 2.23 (3H, s, H-9). The ^{13}C NMR and HSQC spectra confirmed three aromatic carbons (δ_C 121.4, 122.1, 125.4) and one methyl carbon (δ_C 22.1). These data closely match those reported for 2-acetamino-3-hydroxybenzoic acid isolated from *Aspergillus* sp., except for a slight variation in the nitrogen substituent.[36] Key ^{1}H–^{1}H COSY correlations among H-4, H-5, and H-6 corroborated the 1,2,3-trisubstitution pattern. HMBC correlations of H-5/C-1 (δ_C 126.1) and

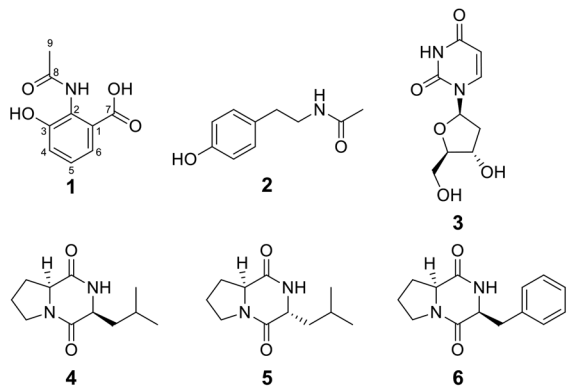

Fig. 1 Chemical structures of isolated compounds **1–6**.

Table 1 ^{1}H (850 MHz) and ^{13}C NMR (212.5 MHz) data of compound **1** in CD_3OD (δ ppm)

Position	δ_C [a], type	δ_H, (J in Hz)
1	126.1, C	
2	126.4, C	
3	149.8, C	
4	121.4, CH	7.05, d (8.0)
5	125.4, CH	7.13, dd (8.0, 7.5)
6	122.1, CH	7.53, d (7.5)
7	171.1, C	
8	171.5, C	
9	22.1, CH_3	2.23, s

[a] ^{13}C NMR data were measured and assigned based on the HSQC and HMBC experiments.

H-6/C-1, H-6/C-7 (δ_C 171.1) confirmed a *meta*-positioned carboxylic acid relative to H-6, while H-9/C-8 (δ_C 171.5) established an acetyl moiety. The molecular formula ($C_9H_9NO_4$) requires two additional heteroatom substituents (–OH and –NH–), one of which is acetylated. HMBC cross-peaks H-4/C-3 (δ_C 149.8) and H-5/C-3 indicate an electron-withdrawing substituent (hydroxyl or amino) at C-3, and further HMBC correlations H-4/C-2 (δ_C 126.4) and H-6/C-2 localize the acetylated group at C-2 (Fig. 2). Thus, two structural isomers were considered: 2-acetamido-3-hydroxybenzoic acid (**1A**) and 2-acetyloxy-3-aminobenzoic acid (**1B**). Conventional 1D and 2D NMR analysis could not unambiguously distinguish these isomers due to their closely similar chemical shifts. Moreover, previously reported ^{1}H NMR data for **1A** differ from our observations, and ^{13}C NMR assignments for **1A** have not been previously disclosed.[36,37] To distinguish between isomers **1A** and **1B** and confirm the positions of the functional groups in compound **1**, we performed NMR chemical shift calculations for both isomers. Using DP4$^+$ probability analysis, the computed ^{1}H and ^{13}C chemical shifts for each isomer were compared with the experimental data for compound **1**. The DP4$^+$ results unambiguously identified compound **1** as isomer **1A**—with the *N*-acetylamine at C-2 and the hydroxyl at C-3—at 100.0% probability (Fig. 2). In addition, linear regression of experimental *versus* calculated ^{13}C shifts yielded an R^2 of 0.9863 for **1A** (Fig. 3), compared to 0.9754 for **1B**, further confirming the accuracy of the **1A** assignment determined by DP4$^+$ analysis.

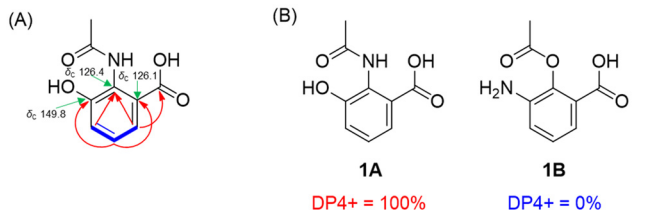

Fig. 2 (A) Key COSY (blue bold) and HMBC (red arrow) correlations for **1** (B) DP4$^+$ analysis and probability scores for **1A**/**1B**.

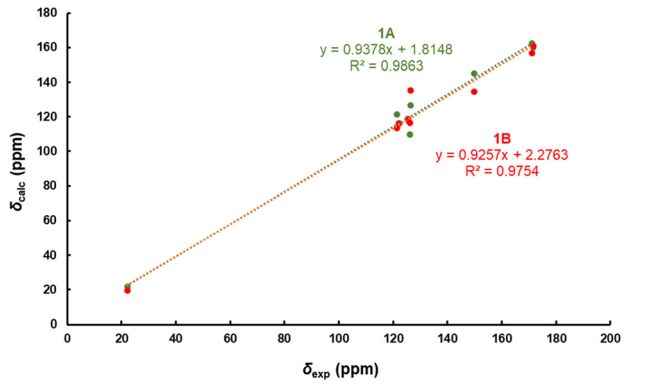

Fig. 3 Regression analysis of experimental *versus* calculated ^{13}C NMR chemical shift of **1A**/**1B** with linear fitting shown as a line.

To further support the structural assignment of compound **1**, we considered its biosynthetic origin. The tryptophan-to-quinolinic acid pathway is well characterized in *Streptomyces* species, in which 3-hydroxyanthranilic acid, the deacetylated core of compound **1**, is a key intermediate.[38] Moreover, *N*-acetylation is a common bacterial modification, frequently observed in *Streptomyces*.[39] From this biosynthetic perspective, compound **1** is more plausibly an anthranilic acid derivative featuring an amide bond than a salicylic acid derivative with an ester linkage. Consequently, the structure of compound **1** was fully elucidated and confirmed as 2-acetamido-3-hydroxybenzoic acid (Fig. 1). To the best of our knowledge, this study provides the first complete ^{13}C NMR assignments for this compound. This compound represents one of several anthranilic acid derivatives produced by *Streptomyces* sp.[40,41]

The remaining isolates were identified as *N*-acetyltyramine (**2**),[42] deoxyuridine (**3**),[42] cyclo(L-Pro-L-Leu) (**4**),[43] cyclo(L-Pro-D-Leu) (**5**),[44] and cyclo(L-Pro-L-Phe) (**6**)[43] (Fig. 1). Their chemical structures were elucidated by comparison of their ^{1}H NMR spectra with previously reported data and LC/MS analysis (Fig. S7-S16).

Evaluation of anti-adipogenic potential of compounds 1–6

To assess the anti-adipogenic potential of compounds **1–6** in differentiated 3T3-L1 cells, we first evaluated their cytotoxicity using the EZ-Cytox assay. Cells were treated with each compound at 1, 50, and 100 μM for 72 h. As shown in Fig. 4, none of the compounds exhibited significant toxicity at concentrations up to 50 μM relative to untreated controls.

Next, we evaluated the effects of compounds **1–6** on lipid droplet formation during 3T3-L1 differentiation. Differentiated cells were fixed with 10% formalin and stained with Oil Red O to visualize intracellular lipids. As illustrated in Fig. 5, treatment with compounds **1–6** (1, 50, and 100 μM) attenuated lipid accumulation in a concentration-dependent manner. Notably, compounds **1**, **2**, and **6** produced significant

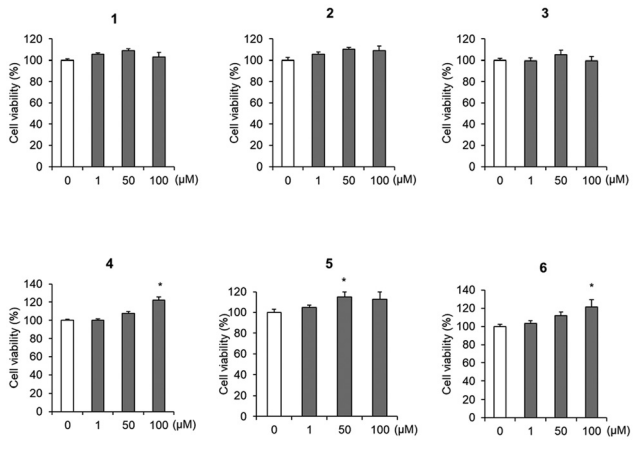

Fig. 4 Effect of compounds **1–6** on cell viability in 3T3-L1 cells. The cells were treated with 0, 1, 50, and 100 μM concentration. Data are presented as mean ± SD (n = 5). Significant differences by Student's t-test (*p < 0.05 *vs.* untreated 3T3-L1 cells).

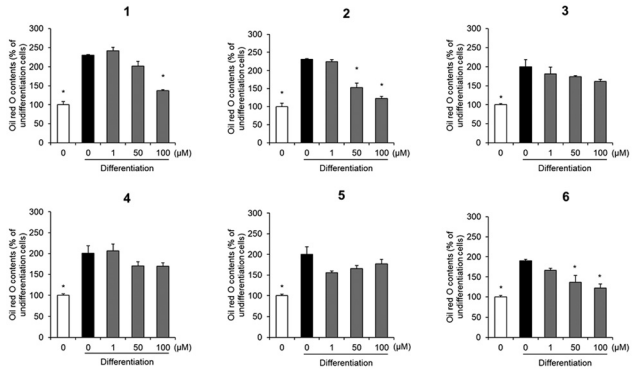

Fig. 5 Effect of compounds **1–6** on adipogenesis of 3T3-L1 cells. The cells were treated with 0, 1, 50, and 100 μM concentration in the presence or absence of differentiation media. The levels of lipid accumulation were quantified by Oil red O staining. Data are presented as mean ± SD (n = 4). * indicates significant differences by Student's t-test (p < 0.05 *vs.* untreated 3T3-L1 cells).

reductions in Oil Red O staining at 50 and 100 μM, whereas compounds **3–5** showed minimal activity. Based on these results, compound **2** was identified as the most potent inhibitor of adipocyte lipid accumulation and was selected for further studies on adipogenic differentiation and the regulation of lipogenic gene expression.

To quantify the impact of compound **2** (50 and 100 μM) on adipogenic regulators and lipogenesis-related genes in differentiated 3T3-L1 adipocytes, we measured mRNA expression by qRT-PCR (Fig. 6). Treatment with compound **2** significantly decreased the transcript level of the master adipogenic transcription factor C/EBPα compared with untreated controls. Furthermore, mRNA levels of SREBP2, FASN, and UCP2—key regulators of lipid synthesis and metabolism—were markedly reduced at both 50 and 100 μM of compound **2**, with the greatest inhibition observed at 50 μM. We also evaluated leptin, an adipokine critical for energy homeostasis, and found its

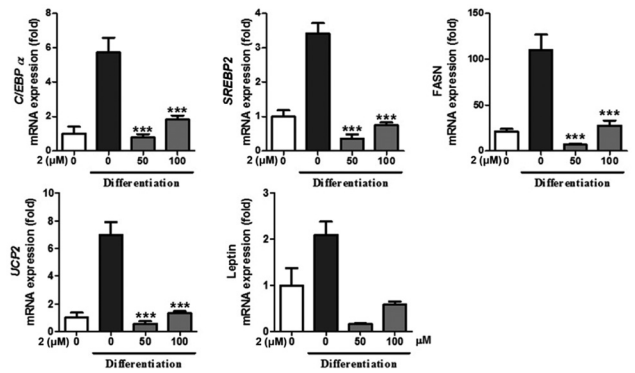

Fig. 6 Effect of compound **2** on the mRNA levels of adipogenic-related factors in 3T3-L1 cells. The mRNA expression levels of C/EBPα, SREBP2, FASN, UCP2, and leptin were measured by qRT-PCR. Relative mRNA expression of each gene was normalized to β-actin in compound **2** treated cells. Data are presented as mean ± SD (n = 4). * indicates significant differences by Student's t-test (p < 0.05 *vs.* untreated 3T3-L1 cells).

expression to be significantly downregulated by compound **2** relative to control cells. Collectively, these results indicate that compound **2** inhibits adipocyte differentiation by down-regulating adipocyte-specific genes, including C/EBPα, SREBP2, FASN, UCP2, and leptin.

3T3-L1 preadipocytes are a well–established *in vitro* model for elucidating the molecular mechanisms of adipogenesis and adipocyte dysfunction in obesity research.[45] Upon hormonal induction, these cells undergo lipid-droplet accumulation and upregulate adipogenic transcription factors such as C/EBP-α, SREBP, and PPAR-γ.[46,47] We therefore employed the 3T3-L1 system to screen six compounds for anti-adipogenic activity. All the isolated compounds (≤100 μM) exhibited no significant cytotoxicity in 3T3-L1 cells; indeed, several treatments modestly increased cell viability, suggesting proliferative effects (Fig. 4). Oil Red O staining of differentiated cells demonstrated that compounds **1–6** (50 and 100 μM) reduced both adipocyte size and lipid deposition, with compound **2** showing the most pronounced inhibition of lipid droplet formation. Given its superior activity, compound **2** was selected for further investigation into its molecular mechanism. During adipogenesis, C/EBP-α functions at the early stage to drive lipid accumulation.[48,49] The treatment of compound **2** markedly downregulated C/EBP-α mRNA, correlating with the reduction in lipid content. Downstream of C/EBP-α, enzymes and regulators of lipogenesis—such as FASN and SREBP2—play critical roles in fatty acid and cholesterol biosynthesis.[50,51] Compound **2** significantly suppressed FASN and SREBP2 expression, indicating interference with both fatty acid synthesis and cholesterol homeostasis. Uncoupling protein 2 (UCP2) modulates mitochondrial fatty acid oxidation and has been implicated in obesity, as UCP2-deficient mice resist high–fat–diet–induced weight gain.[13,52] Consistent with these reports, compound **2** markedly reduced UCP2 mRNA in differentiated adipocytes. Furthermore, compound **2** decreased leptin expression—a key adipokine upregulated during adipocyte maturation and insulin stimulation[53,54]—thereby potentially impacting energy homeostasis.

To date, no studies have directly examined the anti–adipogenic activity of *N*-acetyltyramine (**2**). Previously, *N*-acetyltyramine has been characterized primarily for its antimicrobial effects and as a free radical scavenger.[55,56] Notably, reactive oxygen species (ROS) impair insulin-mediated PI3-kinase/Akt signaling, lipogenesis, and glucose uptake in 3T3-L1 adipocytes; in this context, the radical-scavenging properties of *N*-acetyltyramine may underlie its anti-adipogenic activity.[57,58] By comparison, *p*-hydroxyphenethyl alcohol (tyrosol)—which bears a free hydroxyl in place of the acetamido moiety of compound **2**—attenuates 3T3-L1 differentiation *via* downregulation of adipogenic proteins, reduction of inflammatory mediators, and mitigation of oxidative stress. Moreover, tyrosol has been reported to promote "browning" of white adipose tissue through activation of the AMPK–ATGL–UCP1 axis.[59] In contrast, tyramine (the de-acetylated analogue of compound **2**) mimics insulin action and enhances adipocyte differentiation in 3T3-L1 cells.[60,61] These observations col-

lectively underscore that the terminal functional group on the phenylethyl scaffold critically determines whether the molecule exerts pro- or anti-adipogenic effects.

Conclusion

In this study, we investigated the chemical and biological potential of termite-associated *Streptomyces* sp. M45 and successfully isolated six metabolites (**1–6**) through combined solvent partitioning, RP-C_{18} chromatography, and HPLC purification guided by LC–MS. We fully elucidated the structure of the anthranilic acid derivative **1** *via* comprehensive 1D/2D NMR, HR-ESIMS, and DP4$^+$ analysis, correcting earlier data and providing the first complete ^{13}C NMR assignments. Bioactivity assay in 3T3-L1 adipocytes revealed that, among the isolates, *N*-acetyltyramine (**2**) exhibited the most potent anti-adipogenic effects, significantly reducing lipid accumulation without cytotoxicity. Mechanistic studies demonstrated that compound **2** suppresses adipocyte differentiation by down-regulating key transcription factors (C/EBPα, SREBP2) and lipogenic genes (FASN, UCP2), as well as the adipokine leptin. These findings establish termite-derived *Streptomyces* as a promising source of anti-adipogenic natural products and underscore the critical influence of phenylethyl functionalization on adipogenesis.

Experimental section

General experimental procedures

Ultraviolet–visible (UV–Vis) spectra were recorded on an Agilent 8453 spectrophotometer (Agilent Technologies, Santa Clara, CA, USA). ^{1}H and ^{13}C NMR spectra were acquired on a Bruker AVANCE III HD 850 spectrometer equipped with a 5 mm TCI CryoProbe (Bruker, Karlsruhe, Germany) at 850 MHz (^{1}H) and 212.5 MHz (^{13}C). Chemical shifts (δ) are reported in ppm relative to residual solvent signals (^{1}H: CD_3OD at 3.310 ppm, $CDCl_3$ at 7.260 ppm, and pyridine-d_5 at 8.740 ppm; ^{13}C: CD_3OD at 49.000 ppm) (Cambridge Isotope Laboratories, Tewksbury, MA, USA). Preparative HPLC was performed on a Waters 1525 binary pump coupled to a Waters 996 photodiode array detector (Waters Corporation, Milford, CT, USA) using a Hector-A C_{18} column (250 × 21.2 mm, 5 μm; RStech, Chungcheongbuk-do, Korea) at a flow rate of 5 mL min^{-1}. Semi-preparative separations employed the same HPLC system with a Phenomenex Luna Phenyl-Hexyl column (250 × 10 mm, 10 μm; Phenomenex, Torrance, CA, USA) at 2 mL min^{-1}. Analytical LC–MS analyses were carried out on an Agilent 1200 Series HPLC equipped with a diode array detector and an Agilent 6130 ESI mass spectrometer (Agilent Technologies) using a Kinetex C_{18} column (100 × 2.1 mm, 5 μm; Phenomenex) at 0.3 mL min^{-1}. High-resolution ESIMS data were acquired on an Agilent 6545 Q-TOF mass spectrometer coupled to an Agilent 1290 Infinity II HPLC (Agilent Technologies) with an Eclipse Plus C_{18} column (50 × 2.1 mm, 1.8 μm; Agilent Technologies) at 0.3 mL min^{-1}. Column chromatography was conducted on reversed-phase C_{18} silica gel (230–400 mesh; Merck, Darmstadt, Germany). Thin-layer chromatography was performed on precoated silica gel F_{254} and RP-C_{18} F_{254}s plates (Merck), with visualization under UV light and by heating after spraying with anisaldehyde–sulfuric acid.

Isolation of *Streptomyces* spp

Termite workers of an *Odontotermes* sp. colony were collected in Lajuma, South Africa in 2008, transported in sterile plastic bags, and processed within 24 h of collection. Gut and cuticle tissues were aseptically dissected, and each sample was homogenized in sterile deionized water. The resulting suspensions were spread onto low–nutrient agar plates to promote the growth of oligotrophic bacteria. Colonies displaying filamentous, Actinobacteria–like morphology were picked and restreaked onto ISP2 agar. Successive subculturing on ISP2 agar was performed until pure, axenic Actinobacteria isolates were obtained.

Sequencing and species identification

Genomic DNA from *Streptomyces* sp. M45 was extracted and the 16S rRNA gene was amplified as previously described.[62] The resulting sequence was analyzed for taxonomic identification and submitted to GenBank under accession number SUB15388626.

Isolation of compounds 1–6

Streptomyces sp. M45 was cultivated on sixty ISP-2 agar plates (9 cm diameter) at 30 °C for 14 days. The agar was diced, pooled, and extracted overnight with MeOH. The combined MeOH extract was filtered and concentrated under reduced pressure to yield a crude extract, which was successively partitioned with *n*-hexane, CH_2Cl_2, EtOAc, and *n*-BuOH to afford four fractions: *n*-hexane (752.0 mg), CH_2Cl_2 (155.4 mg), EtOAc (156.9 mg), and *n*-BuOH (1.8 g). The *n*-BuOH fraction (1.8 g) was subjected to reversed-phase C_{18} silica gel column chromatography using a MeOH–H_2O gradient (20 : 80 → 100 : 0, v/v), yielding 12 subfractions (MB1–MB12). Subfraction MB3 (38.8 mg) was purified by semi-preparative HPLC (MeOH–H_2O 20 : 80, v/v, isocratic) to afford compound **1** (t_R 42.5 min, 1.4 mg). The EtOAc fraction (156.9 mg) was fractionated by preparative HPLC with a MeOH–H_2O gradient (10 : 90 → 30 : 70, v/v) into nine subfractions (ME1–ME9). Subfraction ME2 (28.3 mg) was purified by semi-preparative HPLC (MeOH–H_2O 1 : 99, v/v, isocratic) to yield compound **3** (t_R 37.4 min, 1.2 mg). Subfraction ME6 (21.0 mg) was purified by semi-preparative HPLC under isocratic conditions (MeOH–H_2O 19 : 81, v/v) to give compound **2** (t_R 52.0 min, 5.5 mg). The CH_2Cl_2 fraction (155.4 mg) was separated by preparative HPLC using a MeOH–H_2O gradient (40 : 60 → 80 : 20, v/v), yielding eight subfractions (MM1–MM8). Subfraction MM3 (17.0 mg) underwent semi-preparative HPLC (MeOH–H_2O 35 : 65, v/v, isocratic) to furnish compound **4** (t_R 41.3 min, 1.9 mg). Subfraction MM4 (11.8 mg) was similarly purified (MeOH–H_2O 38 : 62, v/v, isocratic) to

isolate compounds **5** (t_R 41.5 min, 1.0 mg) and **6** (t_R 62.5 min, 1.0 mg).

2-Acetamido-3-hydroxybenzoic acid (1)

White amorphous powder; UV (MeOH) λ_{max} ($\log \varepsilon$) 218 (3.8) nm; ^{1}H (850 MHz) and ^{13}C (212.5 MHz) NMR data, see Table 1; HR–ESIMS (positive-ion mode) m/z 196.0597 $[M + H]^+$ (calculated for $C_9H_{10}NO_4$, 196.0604).

Computational NMR chemical shift calculations for DP4$^+$ analysis

DP4$^+$ probability calculations were employed to assign the positions of functional groups in compound **1**. Initial conformational searches were conducted in the OPLS4 force field using MacroModel (v2024-4; Schrödinger LLC, New York, NY, USA) with a mixed torsional/low-mode sampling protocol. All calculations were performed in the gas phase, applying a 20 kJ mol^{-1} energy window and a maximum of 10 000 iterations. The Polak–Ribiere conjugate gradient (PRCG) algorithm was established with 10 000 maximum iterations and a 0.001 kJ (mol Å)$^{-1}$ convergence threshold on the root-mean-square gradient to minimize conformers. The conformers proposed in this study were selected for geometry optimization using TmoleX (version 4.3.2, Turbomole GmbH, Karlsruhe, German), with density functional theory settings of B3-LYP/6-31G(d,p).[63] For each conformer of **1A** (2-acetamido-3-hydroxybenzoic acid; four conformers) and **1B** (2-acetyloxy-3-aminobenzoic acid; six conformers), gauge-invariant atomic orbital (GIAO) magnetic shielding tensors were computed at the B3LYP/6-31G(d,p) level. Calculations were performed within the polarizable continuum model (PCM), and the resulting chemical shifts were Boltzmann-weighted according to the relative population of each conformer. The NMR chemical shifts were derived from the GIAO shielding tensors using the following equation (δ^x_{calc}: calculated ^{1}H/^{13}C NMR chemical shift for nucleus x, σ^o: shielding tensor for the proton/carbon nucleus in tetramethylsilane, σ^x: shielding tensor for the proton/carbon nucleus x).

$$\delta^x_{calc} = \sigma^o - \sigma^x$$

The calculated ^{1}H and ^{13}C NMR chemical shifts were averaged based on their Boltzmann population and used for DP4$^+$ probability calculations using an Excel sheet.[64]

Chemicals for biological activity

Dulbecco's modified Eagle's medium (DMEM) was obtained from Corning (Manassas, VA, USA). Bovine calf serum (BCS) and TRIzol® reagent were acquired from Thermo Scientific (Waltham, MA, USA). Fetal bovine serum (FBS) and penicillin–streptomycin were purchased from Atlas Biologicals (Fort Collins, CO, USA) and Gibco (Grand Island, NY, USA), respectively. Insulin, 3-isobutyl-1-methylxanthine (IBMX), dexamethasone, Oil Red O, isopropanol, and paraformaldehyde solution were supplied by Sigma-Aldrich (St Louis, MO, USA). EZ-Cytox™ assay reagent was provided by DoGen (Seoul, Korea), and AccuPower® qPCR Master Mix was obtained from Bioneer (Daejeon, Korea).

Cell culture and differentiation

The 3T3-L1 mouse preadipocyte cell line was purchased from the American Type Culture Collection (Manassas, VA, USA). Cells were maintained in DMEM supplemented with 10% BCS and 1% penicillin–streptomycin in a humidified incubator at 37 °C with 5% CO_2. Upon reaching approximately 90% confluence, cells were either harvested for assays or induced to differentiate. For adipogenic differentiation, confluent 3T3-L1 preadipocytes were cultured in DMEM containing 10% FBS for 24 h, then treated with differentiation medium (DMEM + 10% FBS) supplemented with 0.5 mM IBMX, 1 μM dexamethasone, 10 μg mL^{-1} insulin, and test compounds for 72 h. Thereafter, cells were maintained in DMEM + 10% FBS containing 10 μg mL^{-1} insulin, with medium changes every 48 h until the completion of differentiation.

Cell viability assay

Preadipocytes were seeded at 1×10^4 cells per well in 96-well plates and allowed to adhere for 24 h. Test compounds (**1–6**) were applied at final concentrations of 0, 1, 50, and 100 μM. After 72 h of treatment, 10 μL of EZ-Cytox reagent was added to each well, and plates were incubated in the dark for 1 h at 37 °C. Absorbance was measured at 450 nm using a PowerWave XS microplate reader (Bio-Tek Instruments, Winooski, VT, USA). Cell viability (%) was calculated relative to untreated controls, which were defined as 100%.

Oil red O staining and quantification

3T3-L1 preadipocytes were plated at 5×10^4 cells per well in 48-well plates and induced to differentiate in the presence of compounds **1–6** (1, 50, and 100 μM). On day 8 post-induction, cells were rinsed twice with Dulbecco's phosphate-buffered saline (DPBS) and fixed in 10% neutral-buffered formalin for 1 h at room temperature. After fixation, cells were washed with DPBS and treated with 60% isopropanol for 5 min to facilitate stain uptake. Cells were then incubated with freshly prepared Oil Red O solution for 20 min, washed four times with distilled water, and air-dried. The retained dye was eluted with 100% isopropanol, and absorbance was measured at 500 nm to quantify intracellular lipid accumulation. Lipid content was expressed as a percentage of the vehicle-treated control (100%).

Gene expression analysis

3T3-L1 cells were plated at 5×10^5 cells per well in 6-well plates and treated with the test compounds throughout differentiation. Total RNA was extracted from differentiated cells using TRIzol® reagent (Thermo Scientific, Waltham, MA, USA) according to the manufacturer's instructions. Total RNA (1 μg) was reverse-transcribed into cDNA using a High-Capacity cDNA Reverse Transcription Kit (Applied Biosystems), and gene expression levels were quantified by quantitative real-time PCR (qRT-PCR)as described.[65]

Statistical analysis

Data are presented as mean ± standard deviation (SD) from at least three independent experiments. One-way ANOVA with a post hoc Tukey's test was performed for statistical comparisons using GraphPad Prism 9 (GraphPad Software, San Diego, CA, USA). Differences were considered statistically significant at $p < 0.05$.

Author contributions

Se Yun Jeong contributed to compound isolations and structural elucidations. Mei Tong He contributed to biological assays. Mihyang Kim and Ki-Hwan Nam contributed to the analysis of biological data. Michael Poulsen contributed to field work, termite sampling, microbial isolation, and edited the manuscript. Christine Beemelmanns contributed to the research project planning and chemical experiments and edited the manuscript. Ki Sung Kang contributed to the research project planning, biological experiments, and manuscript preparation. Ki Hyun Kim contributed to the funding acquisition, research project planning, isolation and chemical analysis, and manuscript preparation.

Conflicts of interest

There are no conflicts to declare.

Data availability

The data supporting this article have been included as part of the SI: UV, MS, HR-ESIMS, NMR spectra of all products. See DOI: **https://doi.org/10.1039/d5ob01062d**.

Acknowledgements

This work was supported by National Research Foundation of Korea (NRF) grants funded by the Korean government (MSIT; grant numbers RS-2019-NR040057 and RS-2021-NR059240).

References

1 J. Jakab, B. Miškić, Š. Mikšić, B. Juranić, V. Ćosić, D. Schwarz and A. Včev, *Diabetes Metab. Syndr. Obes.*, 2021, **14**, 67–83.
2 S. de Ferranti and D. Mozaffarian, *Clin. Chem.*, 2008, **54**, 945–955.
3 J. M. Moreno-Navarrete and J. M. Fernández-Real, *Adipose Tissue Biol.*, 2017, 69–90.
4 D. Moseti, A. Regassa and W.-K. Kim, *Int. J. Mol. Sci.*, 2016, **17**, 124.
5 M. A. Ambele, P. Dhanraj, R. Giles and M. S. Pepper, *Int. J. Mol. Sci.*, 2020, **21**, 4283.
6 C. Janani and B. R. Kumari, *Diabetes Metab. Syndr. Clin. Res. Rev.*, 2015, **9**, 46–50.
7 Y. Zhang, J. Jin, P. Li, H. Yang and Z. Zheng, *Tradit. Med. Res.*, 2022, **7**, 23.
8 J. Zhu, J. Jin, J. Ding, S. Li, P. Cen, K. Wang, H. Wang and J. Xia, *Chem.-Biol. Interact.*, 2018, **290**, 77–87.
9 J. Berndt, P. Kovacs, K. Ruschke, N. Klöting, M. Fasshauer, M. R. Schön, A. Körner, M. Stumvoll and M. Blüher, *Diabetologia*, 2007, **50**, 1472–1480.
10 J. A. Menendez, A. Vazquez-Martin, F. J. Ortega and J. M. Fernandez-Real, *Clin. Chem.*, 2009, **55**, 425–438.
11 T. S. Angeles and R. L. Hudkins, *Expert Opin. Drug Discovery*, 2016, **11**, 1187–1199.
12 T. R. Nagy, M. L. Blaylock and W. T. Garvey, *Nutrition*, 2004, **20**, 139–144.
13 H. J. Kim and J. K. Seong, *BMB Rep.*, 2022, **55**, 500.
14 E. M. Molloy and C. Hertweck, *Curr. Opin. Microbiol.*, 2017, **39**, 121–127.
15 H. Machado, R. N. Tuttle and P. R. Jensen, *Curr. Opin. Microbiol.*, 2017, **39**, 136–142.
16 A. T. Aron, E. C. Gentry, K. L. McPhail, L.-F. Nothias, M. Nothias-Esposito, A. Bouslimani, D. Petras, J. M. Gauglitz, N. Sikora and F. Vargas, *Nat. Protoc.*, 2020, **15**, 1954–1991.
17 C. Beemelmanns, H. Guo, M. Rischer and M. Poulsen, *Beilstein J. Org. Chem.*, 2016, **12**, 314–327.
18 A. A. Visser, T. Nobre, C. R. Currie, D. K. Aanen and M. Poulsen, *Microb. Ecol.*, 2012, **63**, 975–985.
19 T. R. Ramadhar, C. Beemelmanns, C. R. Currie and J. Clardy, *J. Antibiot.*, 2014, **67**, 53–58.
20 E. B. Van Arnam, C. R. Currie and J. Clardy, *Chem. Soc. Rev.*, 2018, **47**, 1638–1651.
21 R. Benndorf, H. Guo, E. Sommerwerk, C. Weigel, M. Garcia-Altares, K. Martin, H. Hu, M. Küfner, Z. W. De Beer and M. Poulsen, *Antibiotics*, 2018, **7**, 83.
22 C. Beemelmanns, T. R. Ramadhar, K. H. Kim, J. L. Klassen, S. Cao, T. P. Wyche, Y. Hou, M. Poulsen, T. S. Bugni and C. R. Currie, *Org. Lett.*, 2017, **19**, 1000–1003.
23 K. F. Chater and D. A. Hopwood, in *Bacillus subtilis and Other Gram–Positive Bacteria*, 1993, pp. 83–99, DOI: **10.1128/9781555818388.ch6**.
24 S. Dharmaraj, *World J. Microbiol. Biotechnol.*, 2010, **26**, 2123–2139.
25 S. Horinouchi and T. Beppu, *Antonie Van Leeuwenhoek*, 1993, **64**, 177–186.
26 J. Distler, K. Mansouri, G. Mayer, M. Stockmann and W. Piepersberg, *Gene*, 1992, **115**, 105–111.
27 S. Serter Kocoglu, M. Secme, C. Oy, G. Korkusuz and L. Elmas, *Antibiotics*, 2023, **12**, 546.
28 H. Matsuo, Y. Kondo, T. Kawasaki and N. Imamura, *Life Sci.*, 2015, **135**, 35–42.
29 J. Yamaguchi, T. Tanaka, H. Saito, S. Nomura, H. Aburatani, H. Waki, T. Kadowaki and M. Nangaku, *Sci. Rep.*, 2017, **7**, 6516.

30 S. Lee, M. Jang, R. Ryoo, J. Roh, S.-K. Ko and K. H. Kim, *Arch. Pharmacal Res.*, 2024, **47**, 272–287.
31 D. E. Lee, K. H. Park, J.-H. Hong, S. H. Kim, K.-M. Park and K. H. Kim, *Arch. Pharmacal Res.*, 2023, **46**, 771–781.
32 T.-Y. Gil, H.-J. Kim, H.-M. Kim, H.-Y. Sim, W. Choi, B. S. Lee, K. H. Kim and H.-J. An, *Nat. Prod. Sci.*, 2024, **30**, 262–267.
33 C. H. Cho, S. H. Chae, S. H. Kim and K. H. Kim, *Nat. Prod. Sci.*, 2024, **30**, 135–142.
34 J.-E. Lee, S. Y. Jeong, Z. Li, H.-Y. Kim, H.-W. Kim, M. J. Yoo, H. J. Jang, D.-K. Kim, N. Cho and H. M. Yoo, *Biomater. Res.*, 2023, **27**, 18.
35 C.-L. You, S.-J. Lee, J. Lee, T. A. Vuong, H.-Y. Lee, S. Y. Jeong, A. Alishir, A. S. Walker, G.-U. Bae and K. H. Kim, *Int. J. Biol. Sci.*, 2023, **19**, 4898.
36 J. Yi, Y. Zhang, X. Wang, C. Wang, C. Sun, J. Wu and Y. Wu, *Phytochem. Lett.*, 2024, **60**, 159–162.
37 H. Hund, A. De Beyer and F. Lingens, *Biol. Chem. Hoppe-Seyler*, 1990, **371**, 1005–1008.
38 O. Kurnasov, V. Goral, K. Colabroy, S. Gerdes, S. Anantha, A. Osterman and T. P. Begley, *Chem. Biol.*, 2003, **10**, 1195–1204.
39 R. M. Burckhardt and J. C. Escalante-Semerena, *Microbiol. Mol. Biol. Rev.*, 2020, **84**, e00090–e00019.
40 Q. Che, L. Qiao, X. Han, Y. Liu, W. Wang, Q. Gu, T. Zhu and D. Li, *Org. Lett.*, 2018, **20**, 5466–5469.
41 M. F. Biabani, M. Baake, B. Lovisetto, H. Laatsch, E. Helmke and H. Weyland, *J. Antibiot.*, 1998, **51**, 333–340.
42 Z.-J. Lin, X.-M. Lu, T.-J. Zhu, Y.-C. Fang, Q.-Q. Gu and W. Zhu, *Arch. Pharmacal Res.*, 2008, **31**, 1108–1114.
43 F. Fdhila, V. Vázquez, J. L. Sánchez and R. Riguera, *J. Nat. Prod.*, 2003, **66**, 1299–1301.
44 M. Adamczeski, A. R. Reed and P. Crews, *J. Nat. Prod.*, 1995, **58**, 201–208.
45 F. J. Ruiz-Ojeda, A. I. Rupérez, C. Gomez-Llorente, A. Gil and C. M. Aguilera, *Int. J. Mol. Sci.*, 2016, **17**, 1040.
46 T.-J. Park, A. Park, J. Kim, J.-Y. Kim, B. S. Han, K.-J. Oh, E. W. Lee, S. C. Lee, K.-H. Bae and W. K. Kim, *BMB Rep.*, 2021, **54**, 124.
47 D. Torres-Villarreal, A. Camacho, H. Castro, R. Ortiz-Lopez and A. L. de la Garza, *J. Physiol. Biochem.*, 2019, **75**, 83–88.
48 V. A. Payne, W.-S. Au, C. E. Lowe, S. M. Rahman, J. E. Friedman, S. O'Rahilly and J. J. Rochford, *Biochem. J.*, 2010, **425**, 215–224.
49 M. Payab, S. Hasani-Ranjbar, M. Baeeri, M. Rahimifard, B. Arjmand, H. Haghi-Aminjan, M. Abdollahi and B. Larijani, *Iran. Biomed. J.*, 2019, **24**, 155.
50 X. Quan, Y. Wang, X. Ma, Y. Liang, W. Tian, Q. Ma, H. Jiang and Y. Zhao, *PLoS One*, 2012, **7**, e33376.
51 E. J. Abente, M. Subramanian, V. Ramachandran and S. H. Najafi-Shoushtari, *Arch. Biochem. Biophys.*, 2016, **589**, 108–119.
52 S. Rousset, M.-C. Alves-Guerra, J. Mozo, B. Miroux, A.-M. Cassard-Doulcier, F. Bouillaud and D. Ricquier, *Diabetes*, 2004, **53**, S130–S135.
53 T. Tsubai, Y. Noda, K. Ito, M. Nakao, Y. Seino, Y. Oiso and Y. Hamada, *Heliyon*, 2016, **2**, e00194.
54 S.-Y. Kim, Y. J. Jang, B. Park, J.-H. Yim, H.-K. Lee, D.-K. Rhee and S. Pyo, *Chem.-Biol. Interact.*, 2016, **257**, 71–80.
55 J. C. Reina, I. Pérez-Victoria, J. Martín and I. Llamas, *Mar. Drugs*, 2019, **17**, 494.
56 B. Heidari and F. Mohammadipanah, *Mol. Biol. Rep.*, 2018, **45**, 2325–2332.
57 Y.-E. Choi, S.-I. Choi, X. Han, X. Men, G.-W. Jang, H.-Y. Kwon, S.-R. Kang, J.-S. Han and O.-H. Lee, *Antioxidants*, 2020, **9**, 1290.
58 S. Furukawa, T. Fujita, M. Shimabukuro, M. Iwaki, Y. Yamada, Y. Nakajima, O. Nakayama, M. Makishima, M. Matsuda and I. Shimomura, *J. Clin. Invest.*, 2017, **114**, 1752–1761.
59 F. Pacifici, C. L. A. Farias, S. Rea, B. Capuani, A. Feraco, A. Coppola, C. Mammi, D. Pastore, P. Abete and V. Rovella, *Oxid. Med. Cell. Longevity*, 2020, **2020**, 4794780.
60 S. Bour, V. Visentin, S. Gres, J. S. Saulnier-Blache, M. Wabitsch and C. Carpéné, *Inflammation Res.*, 2005, **54**, S60–S61.
61 C. Subra, E. Fontana, V. Visentin, X. Testar and C. Carpéné, *J. Physiol. Biochem.*, 2003, **59**, 209–216.
62 H. R. Kang, D. Lee, R. Benndorf, W. H. Jung, C. Beemelmanns, K. S. Kang and K. H. Kim, *J. Nat. Prod.*, 2016, **79**, 3072–3078.
63 S. Y. Jeong, A. Alishir, S. Zhang, Y. Zhang, S. Choi, C. Pang, H. Y. Bae, W. H. Jung and K. H. Kim, *J. Nat. Prod.*, 2023, **86**, 1891–1900.
64 N. Grimblat, M. M. Zanardi and A. M. Sarotti, *J. Org. Chem.*, 2015, **80**, 12526–12534.
65 J.-Y. Kim, S. Jang, H. J. Song, S. Lee, S. Cheon, E. J. Seo, Y. H. Choi and S. H. Kim, *Sci. Rep.*, 2024, **14**, 15064.